Journal of Power Sources 222 (2013) 461–466

Contents lists available at SciVerse ScienceDirect

Journal of Power Sources

journal homepage: www.elsevier.com/locate/jpowsour

Short communication

Self-organized amorphous TiO_2 nanotube arrays on porous Ti foam for rechargeable lithium and sodium ion batteries

Zhonghe Bi [a], M. Parans Paranthaman [a,*], Paul A. Menchhofer [b], Ryan R. Dehoff [b], Craig A. Bridges [a], Miaofang Chi [b], Bingkun Guo [a], Xiao-Guang Sun [a], Sheng Dai [a]

[a] Chemical Sciences Division, Oak Ridge National Laboratory, Oak Ridge, TN 37831, USA
[b] Materials Science and Technology Division, Oak Ridge National Laboratory, Oak Ridge, TN 37831, USA

HIGHLIGHTS

- Self-organized amorphous TiO_2 NTAs have been successfully fabricated on Ti foam.
- TiO_2 NTAs on Ti foam were used as anodes in Li and Na-ion batteries.
- TiO_2 NTAs on Ti foam exhibited improved cycling performance than on Ti foil.
- Self-improving of the specific capacity of Na-ion half cell was occurred during cycling.

GRAPHICAL ABSTRACT

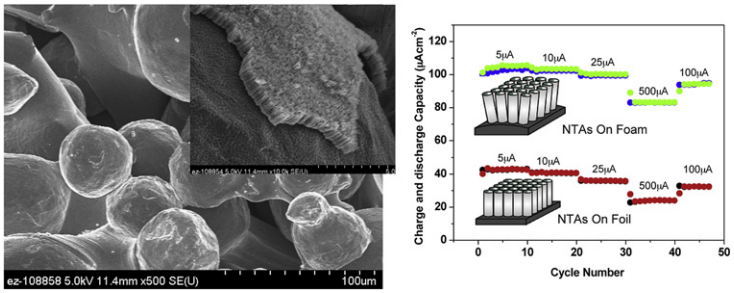

ARTICLE INFO

Article history:
Received 28 May 2012
Received in revised form
4 September 2012
Accepted 5 September 2012
Available online 14 September 2012

Keywords:
TiO_2
Nanotube arrays
Titanium foam
Li-ion
Na-ion
Rechargeable batteries

ABSTRACT

Self-organized amorphous TiO_2 nanotube arrays (NTAs) were successfully fabricated on both Ti foil and porous Ti foam through electrochemical anodization techniques. The starting Ti foams were fabricated using ARCAM's Electron Beam Melting (EBM) technology. The TiO_2 NTAs on Ti foam were used as anodes in lithium ion batteries; they exhibited high capacities of 103 μAh cm^{-2} at 10 μA cm^{-2} and 83 μAh cm^{-2} at 500 μA cm^{-2}, which are two to three times higher than those achieved on the standard Ti foil, which is around 40 μAh cm^{-2} at 10 μA cm^{-2} and 24 μAh cm^{-2} at 500 μA cm^{-2}, respectively. This improvement is mainly attributed to higher surface area of the Ti foam and higher porosity of the nanotube arrays layer grown on the Ti foam. In addition, a Na-ion half-cell composed of these NTAs anodes and Na metal as the counter electrode showed a self-improved specific capacity upon cycling at 10 μA cm^{-2}. These results indicate that TiO_2 NTAs grown on Ti porous foam are promising electrodes for Li-ion or Na-ion rechargeable batteries.

1. Introduction

Rechargeable batteries play an important role in powering mobile or portable electronic devices and in storing energy for green energy systems such as wind and solar [1,2]. Titanium oxide, TiO_2 as anode has the advantage of avoiding solid electrolyte interphase (SEI) formation due to its lithium-ion intercalation voltage and relatively stable cycle performance. In addition, TiO_2 is less toxic and available in high abundance in nature, therefore, it is considered as a replacement for commercial carbon negative electrodes, which suffer from safety concerns due to the formation of lithium dendrites and the SEI layer formation leading to first capacity loss [3]. However, their intrinsic physicochemical property of low electronic conductivity leads to a relatively poor rate

* Corresponding author. Tel.: +1 865 574 5045; fax: +1 865 574 4961.
E-mail address: paranthamanm@ornl.gov (M.P. Paranthaman).

0378-7753/$ – see front matter © 2012 Elsevier B.V. All rights reserved.
http://dx.doi.org/10.1016/j.jpowsour.2012.09.019

capability, which limits its practical industrial application. Recently many efforts have been made to solve this problem of poor rate capability of TiO_2 electrodes. One effective way to increase the electronic conductivity is to modify the bandgap of a pure TiO_2 by different doping schemes to attain enhancement of $[V_O^{\bullet\bullet}]$ and $[h^{\bullet}]$, especially nitrogen-doped anatase TiO_2 exhibited promising performance both in photovoltaic cells and batteries [4–6]. Another efficient way is to use one dimensional TiO_2 nanostructures such as nanowires, nanorods and nanotubes, which not only exhibit large specific surface area, but also provide short diffusion lengths and improved electronic conductivity. In practice, growth of 1D nanostructured TiO_2 on a conducting flexible substrate (Cu or Ti foils) as the electrodes has demonstrated additional advantages: the direct shunting of nanostructured materials to the current-collecting substrate eliminates the use of binders and conducting additives, which improves battery stability and simplifies the battery fabrication process [7,8].

TiO_2 nanowires and nanotubes have been successfully fabricated on Ti foils and used as negative electrode for Li-ion batteries [9–15]. Compared to planar Ti foil, Porous Ti foam provides higher surface area and lighter weight, and the connected 3D frame still maintains high efficiency for the current collection of these nanostructured electrodes. It is reported that bioactive anatase nanotubes fabricated on the porous titanium scaffold have shown obviously improved biocompatibility and apatite-formation ability [16]. Recently, NiO nanocone arrays have also been fabricated by electrodeposition on Ni foam followed by thermal oxidation at 400 °C in air. This binder-free NiO nanocone electrode exhibited excellent performance due to a favorable electrode morphology and enhanced electrical contact between NiO and Ni foam [17,18]. In addition, Xiong et al. reported that amorphous TiO_2 nanotubes with larger diameter on Ti foil are also able to support electrochemical cycling with sodium ions [12]. Therefore, it is interesting to find out whether we can fabricate TiO_2 NTAs on Ti foam as electrodes for Li-ion or Na-ion rechargeable batteries. In the present work, porous Ti foam has successfully been used as substrates for growing TiO_2 NTAs, and this binder- and carbon-free electrode has also been investigated for both Li-ion and Na-ion rechargeable batteries.

2. Experimental

Titanium foam was fabricated using ARCAM's Electron-Beam Melting (EBM) method [19,20], with a thickness of 1.0 mm was cut to 1 × 5 cm^2 and cleaned ultrasonically in water, ethanol and acetone for 5 min, consequently, and finally dried in Ar. A two-electrode electrochemical anodization cell with a platinum cathode was used to grow the nanotubes in 0.1 M NH_4F (H_2O:EG (Ethylene Glycol) = 20:80 in volume) under a constant voltage of 40 V for 1.5 h [21]. The temperature of the electrolyte bath was maintained at 15 °C by a chiller with coolant cycling. For comparison, the same procedure was applied to Ti foils (1 × 5 cm^2) (Alfa Aesar, 99.5%). The morphology, microstructure, and phase structure of the grown nanotube arrays were examined with a Hitachi S-4800 FEG scanning electron microscope (SEM) and a Scintag PAD X-ray diffractometer (XRD) employing Cu Kα radiation.

The two-electrode electrochemical test cells were assembled in an argon-filled glove box using nanotube arrays on Ti foil and ARCAM Ti foam (without binders and conducting carbon), as the working electrode and metallic lithium foil or sodium pellets as the counter electrode. The NTAs on the back side of the substrates were scratched off to provide a good contact for current collection. The electrolyte for Li-ion batteries consisted of a solution of 1 M $LiPF_6$ in ethylene carbonate (EC)/dimethyl carbonate (DMC)/diethyl carbonate (DC) (1:1:1 by volume). For Na-ion batteries, an electrolyte composition of 1 M $NaClO_4$ in EC/DMC (1:1) was used. An active mass of nanotubes was estimated from the amount of nanotubes removed from the foil by scratching and assuming symmetric mass distribution on the titanium foil. However, the area capacity was used for NTAs on Ti foam since active mass of the nanotubes could not be estimated on the Ti foam where it is impossible to fully remove the nanotubes from the porous substrates to calculate the mass of tubes. Galvanostatic charge/discharge cycling between the voltages of 1.0–2.5 V was performed at room temperature under different rates using an Arbin potentiostat/galvanostat multichannel system. Cyclic voltammetry was performed on a VersaSTAT 3 (Princeton Applied Research) electrochemical workstation.

3. Results and discussion

SEM images of the Ti foam substrate before and after anodization under a constant potential of 40 V at 15 °C for 1.5 h are shown in Fig. 1(a) and (b), respectively. It can be seen that where the film has not broken off during handling the Ti foam substrate was uniformly covered with TiO_2 NTAs as shown in Fig. 1(b). In addition to anodic oxidation, similar electrodeposition methods can also be utilized to coat any surface geometry with simple surface preparation [18,22]. Fig. 1(c) and (e) shows the SEM images of the cross-section and top view of TiO_2 NTAs on the Ti foam, respectively. It can be observed that the average length of the nanotubes is around 1.5 μm and the diameters of the nanotubes vary from 80 to 150 nm. It should also be noted that the diameter of nanotubes formed on the Ti foam is not as uniform as on the Ti foil. This variability is probably due to the simple factor that the surface of the Ti foam is not as smooth as the surface on the Ti foil. Comparing the NTAs layer formed on the Ti foil via the top-view and cross-section view, as shown in Fig. 1(d) and (f), a compact NTAs layer was formed on the Ti foil. The average diameter and the length of the nanotubes on the Ti foil are 100 nm and 3.0 μm, which is much longer than the nanotubes on the foam. It is not clear that the TiO_2 nanotubes on Ti foam grew more slowly than on Ti foil. However, increased spacing observed between the nanotubes on the Ti foam clearly indicates a slightly lower nanotube density at their ends with respect to their origin on the Ti foam substrates. This is likely due to the fact that the nanotube orientation develops perpendicular to the rough and curved surface of the Ti foam substrates (see the inserted schematics in Fig. 1(e) and (f)). This increased spacing is somewhat advantageous, as the greater volume of electrolyte solution between the tubes facilitates delivery of Li^+ ions to the tube walls. Furthermore, the shorter length of the nanotubes on Ti foam also probably provides a thinner insulator layer compared to that on the foil. The as-prepared TiO_2 nanotube arrays on both Ti foam and Ti foil are amorphous as determined by XRD (see Fig. 2). Only peaks from Ti were observed in the XRD patterns of the as-formed TiO_2 NTAs; however, after annealing at 300 °C in 4% H_2/Ar for 1 h, crystalline anatase TiO_2 phase was observed both on the Ti foil and foam.

Fig. 3 shows cyclic voltammetry (CV) of the NTAs electrode at a scan rate of 0.1 mV s^{-1} on the Ti foil (a) and the Ti foam (b), respectively. Amorphous TiO_2 electrodes were used in electrochemical testing, as annealing affected the tube morphology and previous studies of the cycling of amorphous TiO_2 have shown better performance than crystalline TiO_2 [10]. A very broad band in the range of 1.4–2.5 V during cycling is observed for the NTAs electrode on the Ti foil in Fig. 3(a), which is similar to a previous study on TiO_2 nanotubes [10]. For the NTAs on Ti foam, however, more obvious pseudocapacitative behavior can be seen in Fig. 3(b) since Ti foam provides higher surface area and a porous TiO_2 NTAs layer. The NTAs electrodes on different substrates were also

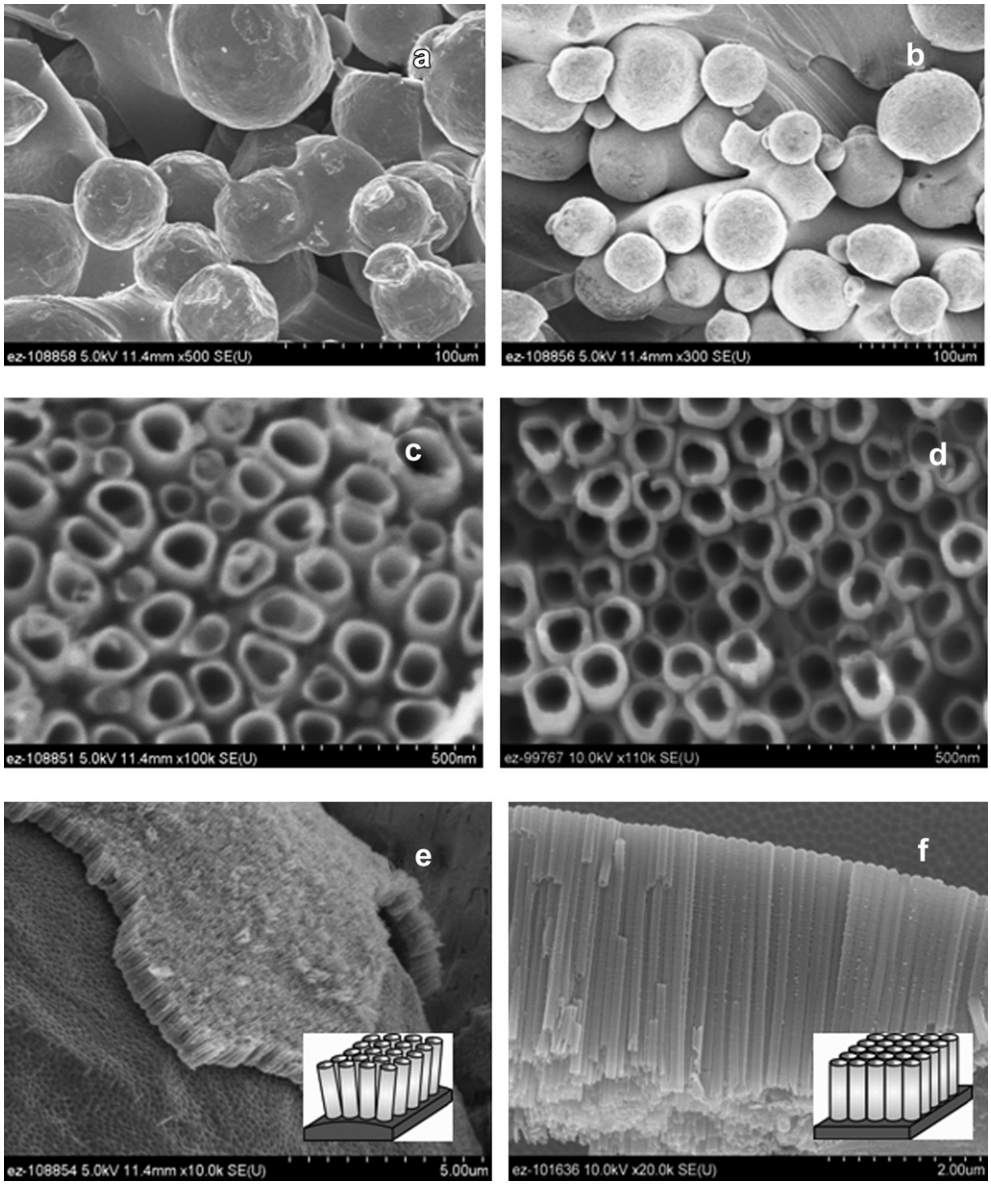

Fig. 1. SEM images of the Ti foam before (a) and after (b) anodized; Top views of the as-prepared TiO_2 NTAs on the Ti foam (c) and Ti foil (d) substrates; Cross-section view of the as-prepared TiO_2 NTAs on the Ti foam (e) and Ti foil (f) substrates. Pictures inserted in (e) and (f) are the schematics of the TiO_2 NTAs grown on the surface of Ti foam (left) and Ti foil (right), respectively.

examined by means of galvanostatic measurements, allowing direct comparison in the performance. Fig. 4 shows the galvanostatic discharge/charge curves of the NTA electrodes on the Ti foil (a) and Ti foam (b), between 2.5 and 1.01 V at a rate of 10 μA cm^{-2} (C/4 for TiO_2 NTAs on the foil). During the first discharge, the voltage pseudoplateau near 1.1 V contributes to a large irreversible capacity. The first discharge capacity for the NTAs electrode on Ti foil is 74 μAh cm^{-2} (278 mAh g^{-1}), and a reversible charge capacity of 52 μAh cm^{-2} (195 mAh g^{-1}) was achieved after the first discharge, leading to an irreversible capacity of 22 μAh cm^{-2}. For the NTAs electrode on Ti foam, a first discharge capacity of 130 μAh cm^{-2} and a reversible capacity of 93 μAh cm^{-2} were obtained, which are much higher than those of the NTAs on foil. They both exhibited initial coulombic efficiencies of ~71%, which agrees with previously published reports [10,11]. Fig. 5(a) shows the cycling performance of the NTAs electrodes on Ti foil and foam at 10 μA cm^{-2}. The NTAs electrode on Ti foil exhibited a reversible capacity of 40.6 μAh cm^{-2} in the second cycle, which maintained at 39.6 μAh cm^{-2} after 100 cycles with a high coulombic efficiency. For NTAs electrode on Ti foam, a reversible capacity of 95 μAh cm^{-2} was achieved in the second cycle, which gradually increased to 102 at the 20th cycle and then maintained at a capacity of ~101 μAh cm^{-2} after 100 cycles with a high coulombic efficiency. The TiO_2 nanotube electrodes formed both on foil and foam showed the absence of voltage plateaus in the CV curves since all of them are amorphous, in which the considerable disordered structures and defects present will not only create large spatial channels for Li-ion diffusion, but also provide many sites for Li-ion insertion at relatively higher potential during discharging [23].

The rate capabilities of the NTAs electrodes on Ti foil and foam have been evaluated at various rates ranging from 5 to 500 μA cm^{-2}. The results are shown in Fig. 5(b). Under the low current rate of 5 μA cm^{-2}, the charge capacities are close to 43 μAh cm^{-2} for Ti foil and 105 μAh cm^{-2} for Ti foam after 10 cycles.

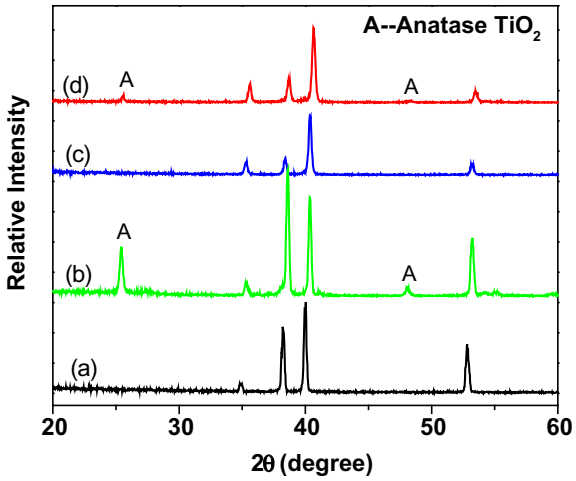

Fig. 2. X-ray diffraction patterns of TiO_2 NTAs on different substrates obtained at 15 °C ((a) as prepared on foil, (b) annealed on foil, (c) as prepared on foam, (d) annealed on foam).

With increasing charge–discharge rate, the charge capacity of the NTAs electrode on Ti foil slightly reduced to 40, 35, and 32 μAh cm^{-2} at rates of 10, 25, 100 μA cm^{-2}, respectively. For the NTAs on Ti foam, however, the charge capacity reduced to 103, 100

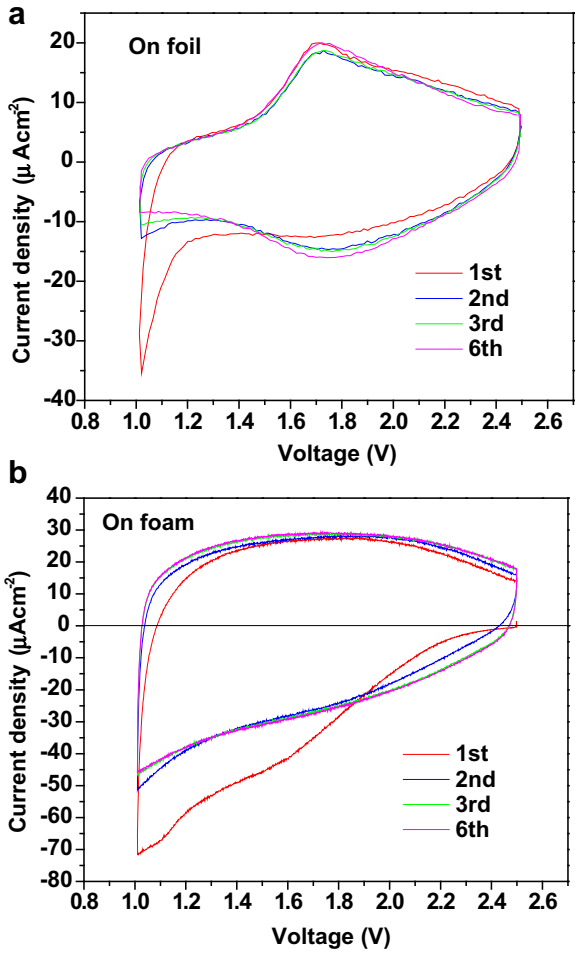

Fig. 3. Cyclic voltammetry curves of TiO_2 NTAs on the different substrates (a) Ti foil and (b) Ti foam at a scan rate of 0.1 mV s^{-1} between 1.01–2.5 V.

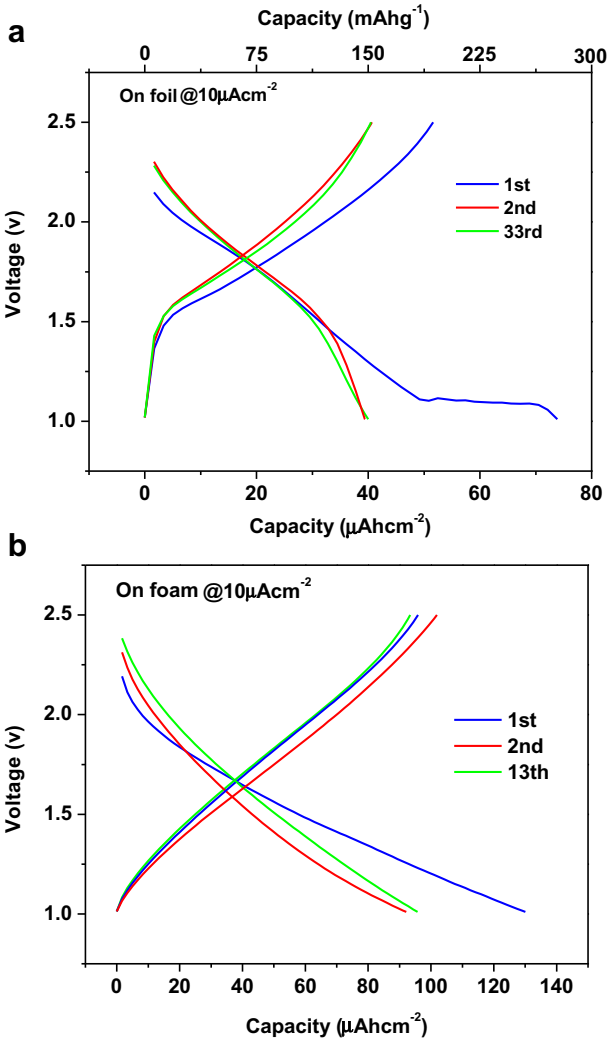

Fig. 4. Discharge and charge curves of TiO_2 NTAs on (a) Ti foil and (b) Ti foam in Li-ion half-cells.

and 94 μAh cm^{-2} at rates of 10, 25, and 100 μA cm^{-2}, respectively. Especially at the rate as high as 500 μA cm^{-2}, the NTAs on Ti foam showed a charge capacity of 83 μA cm^{-2}, which is much higher than that on Ti foil, which is only around 24 μAh cm^{-2}. As shown in the above cycling and rate performance, the NTAs electrodes prepared both on Ti foil and Ti foam exhibited great cycling stability for Li-ion rechargeable batteries. The higher capacity and better rate performance of the NTAs electrode was achieved on Ti foam, probably due to the presence of higher surface area, shorter tube length, and higher porosity than that on Ti foil, which are beneficial to improve the transportation of Li-ion on the TiO_2 electrode. For example, the surface area of the Ti foam could be estimated and calculated from the SEM images while the same dimension of foil and foam were used. We hypothesized that the Ti foam is composed of spheres with an average diameter of 50 μm. Compared to the same dimensions of foil (1 cm × 1 cm × (different thicknesses of 0.05–1.0 mm)), the surface area for the Ti foam is around 1.5–30 cm^2 for different thicknesses, however, the surface area of the foil is only around 2.0–2.2 cm^2.

In addition, amorphous TiO_2 nanotubes on Ti foam were also investigated as an anode for rechargeable sodium ion batteries. Fig. 6(a) shows galvanostatic charge and discharge curves of amorphous TiO_2 NTAs on Ti foam in a Na half-cell cycled between

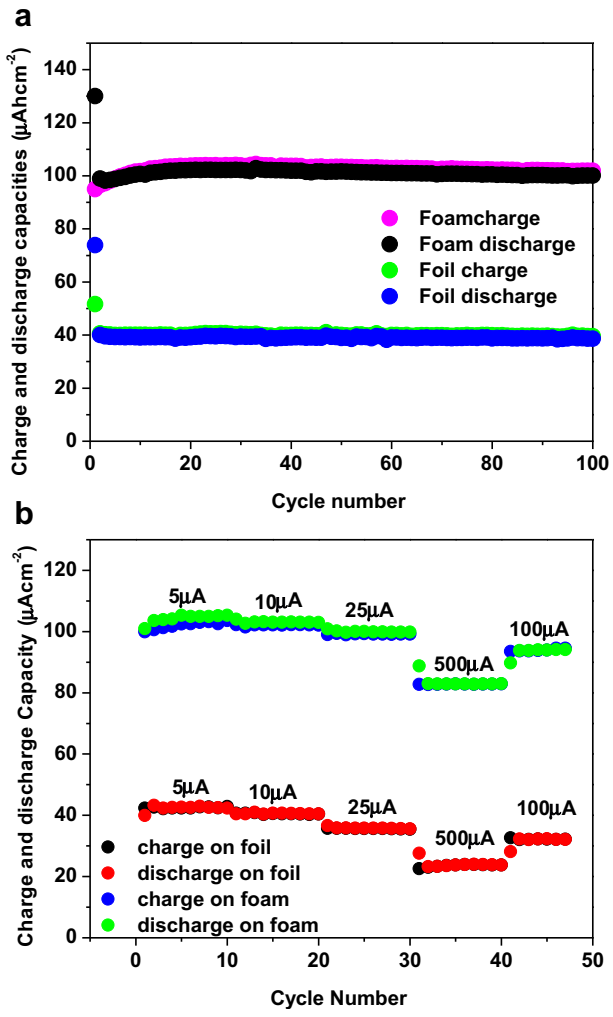

Fig. 5. (a) Cyclic performance of the TiO_2 NTAs on the Ti foil and foam in Li-ion half-cells at a current density of 10 μA cm^{-2}. (b). Cycle performance of TiO_2 NTAs on Ti foil and foam at various charge and discharge rates.

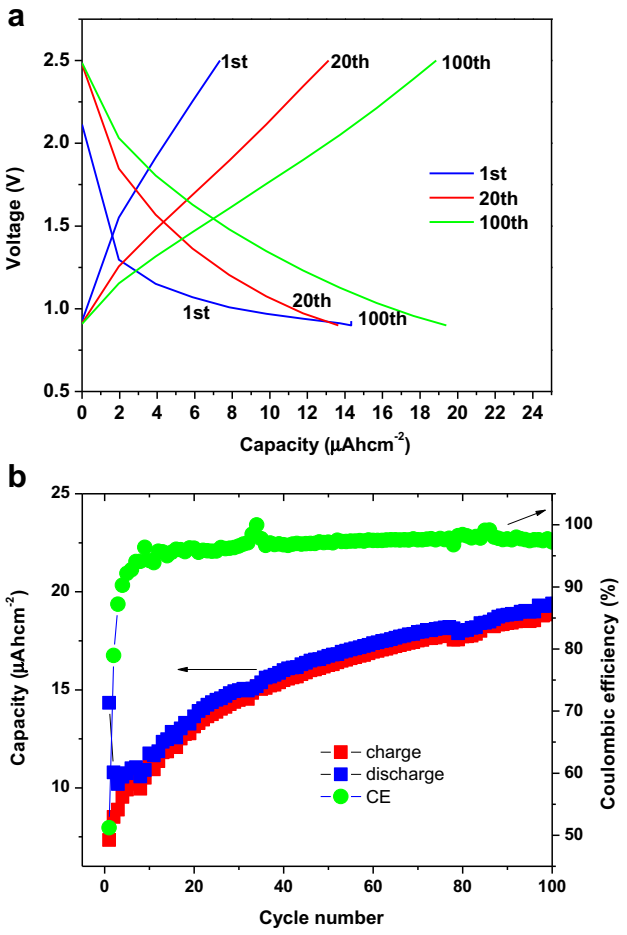

Fig. 6. Electrochemical characterization of TiO_2 NTAs on Ti foam in a Na-ion half-cell. (a) Charge/discharge galvanostatic curves of amorphous TiO_2 NTAs in Na-ion half cell cycled between 2.5 and 0.9 V versus Na/Na+ at 10 μA cm^{-2}. (b) Capacity and coulombic efficiency vs. cycle number measured at a current density of 10 μA cm^{-2} in Na half cell.

2.5 and 0.9 V versus Na/Na^+ at a rate of 10 μA cm^{-2}. One pseudo-plateau near 1.10 V was also observed in the first cycle (Fig. 6(a)), which contributes to a large irreversible reaction of Na, leading to a total capacity of 14.3 μAh cm^{-2}. A reversible capacity of 7.3 μAh cm^{-2} was attained after the first cycle with a coulombic efficiency of 51%, which is significantly lower than the initial coulombic efficiency of 71% observed for Li-ion based NTA batteries. Fig. 6(b) shows that the coulombic efficiency of Na-ion based batteries becomes higher than 95% after 7 cycles. Similar self-improving behavior was continually observed even up to 100 cycles. From Fig. 6(b), the capacity almost doubled to reach 13.6 μAh cm^{-2} after 20 cycles and tripled to reach 19.4 μAh cm^{-2} after 100 cycles, respectively. The increase in capacity may be related to an electrochemically driven transformation of amorphous TiO_2 nanotubes into a face-centered-cubic crystalline phase [24]. For the Li-ion system, however, self-improvement of the specific capacity was only observed at fast cycling of 3 A g^{-1}, due to the presence of different ion sizes and salvation energy [12]. The Li ions are easy to infiltrate into pores in high concentration since Li ion exhibits the largest adsorption [25]. Indeed, it was previously observed that Li ions adsorb strongly on the TiO_2 surface in aprotic electrolyte solutions, where no adsorption of Na ions was observed under the same conditions [26]. Therefore, at low cycling rate, Na ion first needs to diffuse into the interior of the pores of TiO_2 nanotubes in a relatively high concentration, then diffuse into the TiO_2 matrix, which will lead to the self-improvement of the capacity in the Na-ion system as observed at a slower cycling rate. For the Li-ion system, however, large amounts of Li ions is already present in the pores because of the large Li adsorption at the surface, therefore, the self-improvement of the capacity in Li system only occurs at a higher cycling rate. These NTAs on porous Ti substrates indeed hold promise for the future development of Li or Na-ion battery systems.

4. Conclusions

In summary, well-ordered amorphous TiO_2 NTAs have been successfully fabricated on porous Ti foam. These porous structures not only provide good electrical contact between the active materials and the current collector, but also more surface area for growing NTAs as compared to Ti foil. As a result, a greater storage capacity is possible for a given electrode area with Ti foam. In addition, the TiO_2 NTAs grown on Ti foam exhibits higher porosity than on Ti foil under the same conditions. These advantages of the TiO_2 NTAs on Ti foam provide a straightforward approach to improve the performance of Li-ion or Na-ion rechargeable batteries.

Acknowledgment

This work was sponsored by the Materials Science and Engineering Division, Office of Basic Energy Sciences, U.S. Department of Energy. Microscopy work was conducted at the ORNL SHaRE user facility, which is sponsored by the Office of Basic Energy Sciences, U.S. Department of Energy. Dr. M. Chi was supported by the ORNL LDRD Seed Funding LOIS # 5902. Drs. Z. Bi and B. Guo acknowledge the support of the ORISE postdoctoral fellowship.

References

[1] M. Winter, R.J. Brodd, Chem. Rev. 104 (2004) 4245.
[2] B. Dunn, H. Kamath, J.M. Tarascon, Science 334 (2011) 928.
[3] Z.G. Yang, D. Choi, S. Kerisit, K.M. Rosso, D.H. Wang, J. Zhang, G. Graff, J. Liu, J. Power Sources 192 (2009) 588.
[4] M. Batzill, E.H. Morales, U. Diebold, Phys. Rev. Lett. 96 (2006) 026103.
[5] K.S. Han, J.W. Lee, Y.M. Kang, J.Y. Lee, J.K. Kang, Small 4 (10) (2008) 1682.
[6] H.K. Han, T. Song, J.Y. Bae, L.F. Nazar, H. Kim, U. Paik, Energy Environ. Sci. 4 (2011) 4532.
[7] D.V. Bavykin, F.C. Walsh, Eur. J. Inorg. Chem. 8 (2009) 977.
[8] X. Su, Q.L. Wu, X. Zhan, J. Wu, S.Y. Wei, Z.H. Guo, J. Mater. Sci. 47 (2012) 2519.
[9] K. Wang, M. Wei, M.A. Morris, H. Zhou, J.D. Holmes, Adv. Mater. 19 (2007) 3016.
[10] G.F. Ortiz, I. Hanzu, T. Djenizian, P. Lavela, J.L. Tirado, P. Knauth, Chem. Mater. 21 (2009) 63.
[11] B. Liu, D. Deng, J.Y. Lee, E.S. Aydil, J. Mater. Res. 25 (2010) 1588.
[12] H. Xiong, M.D. Slater, M. Balasubramanian, C.S. Johnson, T. Rajh, J. Phys. Chem. Lett. 2 (2011) 2560.
[13] G.K. Mor, O.K. Varghese, M. Paulose, N. Mukherjee, C.A. Grimes, J. Mater. Res. 18 (2003) 2588.
[14] Z. Su, W. Zhou, Adv. Mater. 20 (2008) 3663.
[15] J. Tao, J. Zhao, X. Wang, Y. Kang, Y. Li, Electrochem. Commun. 10 (2008) 1161.
[16] X.P. Fan, B. Feng, J. Weng, J.X. Wang, X. Lu, Mater. Lett. 65 (2011) 2899.
[17] Q. Pan, J. Liu, J. Solid State Electrochem. 13 (2009) 1591.
[18] X.H. Wang, Z. Yang, X. Sun, X. Li, D. Wang, P. Wang, D. He, J. Mater. Chem. 21 (2011) 9988.
[19] P. Heinl, C. KÖrner, R.F. Singer, Adv. Eng. Mater. 10 (2008) 1.
[20] M. Koike, P. Greer, K. Owen, G. Lilly, L.E. Murr, S.M. Gaytan, E. Martinez, T. Okabe, Materials 4 (2011) 1776.
[21] X. Qiu, J. Howe, M. Cardoso, O. Polat, W. Heller, M. Paranthaman, Nanotechnology 20 (2009) 455601.
[22] Z. Bi, J. Zhu, J. Batey, J. Power Sources 195 (2010) 3605.
[23] D.S. Guan, C. Cai, Y. Wang, J. Nanosci. Nanotechnol. 11 (2011) 3641.
[24] H. Xiong, H. Yildirim, E.V. Shevchenko, V.B. Prakapenk, B. Koo, M.D. Slater, M. Balasubramanian, S.K. Sanaranarayanan, J.P. Greeley, S. Tepavcevic, N.M. Dimitrijevic, P. Podsiadlo, C.S. Johnson, T. Rajh, J. Phys. Chem. C 116 (2012) 3181.
[25] A. Wynveen, F. Bresme, J. Chem. Phys. 133 (2010) 10.
[26] J. Wang, J. Polleux, J. Lim, B. Dunn, J. Phys. Chem. C 111 (2007) 14925.